Inorganic Chemistry

Article

pubs.acs.org/IC

Reactivity of Cys_4 Zinc Finger Domains with Gold(III) Complexes: Insights into the Formation of "Gold Fingers"

Aurélie Jacques,[†,‡,§] Colette Lebrun,[⊥,∥] Angela Casini,[¶] Isabelle Kieffer,[≠,#] Olivier Proux,[≠,#] Jean-Marc Latour,*[,†,‡,§] and Olivier Sénèque*[,†,‡,§]

[†]Université Grenoble Alpes, LCBM/PMB, F-38000 Grenoble, France

[‡]CNRS, LCBM/PMB, UMR 5249, F-38000 Grenoble, France

[§]CEA, IRTSV-LCBM, PMB, F-38000 Grenoble, France

[⊥]Université Grenoble Alpes, INAC-SCIB, F-38000 Grenoble, France

[∥]CEA, INAC-SCIB, F-38000 Grenoble, France

[¶]Department of Pharmacokinetics, Toxicology and Targeting, Research Institute of Pharmacy, University of Groningen, A. Deusinglaan 1, 9713 AV Groningen, The Netherlands

[≠]BM30B/FAME beamline, European Synchrotron Radiation Facility (ESRF), F-38000 Grenoble, France

[#]Observatoire des Sciences de l'Univers de Grenoble, UMS 832, CNRS, Université Joseph Fourier, F-38000 Grenoble, France

ABSTRACT: Gold(I) complexes such as auranofin or aurothiomalate have been used as therapeutic agents for the treatment of rheumatoid arthritis for several decades. Several gold(I) and gold(III) complexes have also shown in vitro anticancer properties against human cancer cell lines, including cell lines resistant to cisplatin. Because of the thiophilicity of gold, cysteine-containing proteins appear as likely targets for gold complexes. Among them, zinc finger proteins have attracted attention and, recently, gold(I) and gold(III) complexes have been shown to inhibit poly(adenosine diphosphate ribose)polymerase-1 (PARP-1), which is an essential protein involved in DNA repair and in cancer resistance to chemotherapies. In this Article, we characterize the reactivity of the gold(III) complex $[Au^{III}(terpy)Cl]Cl_2$ (Auterpy) with a model of $Zn(Cys)_4$ "zinc ribbon" zinc finger by a combination of absorption spectroscopy, circular dichroism, mass spectrometry, high-performance liquid chromatography analysis, and X-ray absorption spectroscopy. We show that the $Zn(Cys)_4$ site of $Zn{\cdot}L_{ZR}$ is rapidly oxidized by Auterpy to form a disulfide bond. The Zn^{2+} ion is released, and the two remaining cysteines coordinate the Au^+ ion that is produced during the redox reaction. Subsequent oxidation of these cysteines can take place in conditions of excess gold(III) complex. In the presence of excess free thiols mimicking the presence of glutathione in cells, mixing of the zinc finger model and gold(III) complex yields a different product: complex $(Au^I)_2{\cdot}L_{ZR}$ with two Au^+ ions bound to cysteines is formed. Thus, on the basis of detailed speciation and kinetic measurements, we demonstrate herein that the destruction of $Zn(Cys)_4$ zinc fingers by gold(III) complexes to achieve the formation of "gold fingers" is worth consideration, either directly or mediated by reducing agents.

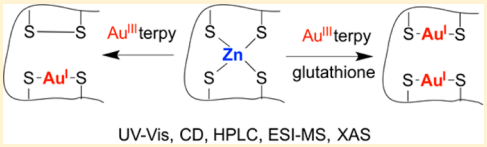

INTRODUCTION

Gold(I) complexes have been used for several decades in the treatment of rheumatoid arthritis, a chronic autoimmune disease that is characterized by inflammatory processes at joints and leads to joint erosion.[1] Active compounds used as treatment are gold(I) thiolates such as Myocrisin (sodium aurothiomalate) or auranofin [triethylphosphinegold(I) tetraacetylthioglucose] (Figure 1).[2,3] They decrease the inflammatory process and slow down the progression of the disease. In the 1980s, it was shown that auranofin inhibited the growth of cancer cells in vitro but with limited activity in vivo.[4,5] This has prompted the synthesis and evaluation of the properties of new gold(I) complexes as anticancer agents.[2,3,6−8] In concomitance, based on the success of platinum(II) complexes such as cisplatin regarding cancer treatments, gold(III) complexes isoelectronic with platinum(II) were investigated as antitumor agents and often showed high cytotoxicity toward cancer cells.[2,3,6−8] Intensive research is still ongoing with new classes of gold(III) complexes,[9] and several proteins have been identified as possible pharmacological targets.[2,10−12] Among them, it is worth mentioning the selenoenzyme thioredoxin reductase,[13] cathepsins,[14,15] tyrosine phosphatases,[16,17] mem-

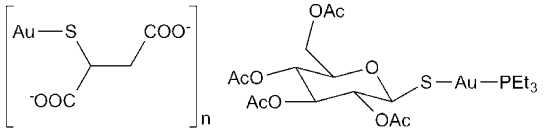

Figure 1. Gold(I) complexes used as therapeutic agents.

Received: February 13, 2015
Published: April 3, 2015

DOI: 10.1021/acs.inorgchem.5b00360
Inorg. Chem. 2015, 54, 4104−4113

brane protein water/glycerol channels (aquaporins),[18,19] and transcription factors.[20,21] Most of these targets possess free cysteine residues that can bind gold, leading to enzyme/protein inhibition. Within this frame, the interaction of gold complexes with copper-trafficking proteins was also demonstrated. It was shown that gold(I) is able to bind to *apo*-CueR,[22] a regulator of copper homeostasis in bacteria, and to *apo*-Atox-1, a human copper chaperone,[23] and that cellular uptake of gold(I) complexes in melanoma cells occurs mainly via Ctr1, a transmembrane protein harnessing several methionines and cysteines to import Cu^+ into the cytoplasm.[24,25]

It has also been reported that gold complexes can interact with cysteine residues of zinc fingers. Zinc fingers are small protein domains playing a structural role by ensuring the proper fold of a protein.[26−32] In zinc finger sites, a Zn^{2+} ion is coordinated in tetrahedral geometry by a combination of histidine and/or cysteine residues, forming three possible arrangements, namely, Cys_2His_2, Cys_3His, and Cys_4. Proteomic studies have estimated to ca. 3000 the number of zinc proteins in human genome, and among them, the majority are zinc finger proteins.[33−35] Zinc fingers have different functions (they can be pure structural elements, mediate protein/DNA, protein/RNA, or protein/protein interactions, act as redox switches, or catalyze alkyl transfer reactions), different folds, and different biological locations.[27,36−39] Several classifications of zinc finger domains based mainly on their fold and their biological role have emerged in the literature during the past years.[28−31,39] They led to identification of at least 14 classes of zinc fingers.[39] Potential interaction between gold(I) complexes and zinc finger transcription factors is of high interest because several zinc finger proteins (Egr-1[40,41] and tristetraproline[42]) regulate the expression of TNF-α, the major proinflammatory cytokine involved in rheumatoid arthritis. In this regard, the antiarthritis drug aurothiomalate (Figure 1) inhibits DNA binding of nuclear receptors, which are zinc finger transcription factors, and gene expression.[43,44] At a molecular level, it was shown by the combination of electrospray ionization mass spectrometry (ESI-MS) and circular dichroism (CD) that the reaction of aurothiomalate with the third zinc finger of Sp1 (a classical $\beta\beta\alpha$ zinc finger) leads to the replacement of Zn^{2+} by one Au^+ ion and conformational changes.[45] Moreover, it was estimated that this classical $\beta\beta\alpha$ Cys_2His_2 zinc finger transcription factor has an apparent 4-fold higher affinity for Au^+ compared to Zn^{2+}. Binding of gold(I) originating from $[Au(PEt_3)(Cl)]$ was also demonstrated with the apo forms of the three variants (Cys_2His_2, $Cys_2HisCys$, and Cys_4) of the consensus peptide of classical $\beta\beta\alpha$ zinc fingers.[46]

Concerning gold(III) complex interactions with zinc fingers, gold(III) compounds containing diethylenetriamine and 2,2′,2″-terpyridine ligands were reported to react with the second zinc finger of HIV nucleocapsid protein, a $Cys_2HisCys$ zinc finger, leading to the release of Zn^{2+} and the formation of Au_2-peptide and Au_4-peptide adducts as detected by ESI-MS experiments.[47] The reduction of Au^{3+} to Au^+ was proposed, but not demonstrated, based on the additional observation of oxidized peptide with disulfide bonds. Moreover, gold(III) complexes such as auphen $[Au^{III}(phen)Cl^+_2$, where phen = 1,10-phenanthroline] were reported to inhibit poly(adenosine diphosphate ribose)polymerase-1 (PARP-1),[48] which is an essential protein involved in DNA repair and in cancer resistance to chemotherapies. High-resolution mass spectrometry (HRMS) allowed one to establish that gold(III) complexes react with the zinc finger site of PARP-1 (treble clef $Cys_2HisCys$ zinc finger domain), leading to the release of Zn^{2+}, binding of Au^{3+} to the peptide with the release of the phen ligand, and oxidation of two cysteines into a disulfide when the gold compound is reacted directly with *apo*-PARP-1. These results support a model whereby displacement of zinc from the PARP-1 zinc finger by Au ions leads to decreased PARP-1 activity and to formation of the so-called "gold finger" domain.

Very recently, Casini et al. applied HRMS to investigate the interactions of auphen and auranofin with a Cys_2His_2 model zinc finger peptide (classical $\beta\beta\alpha$).[49] In addition, a hybrid quantum mechanics/molecular mechanics approach was used to determine the effects of binding of Au^+ and Au^{3+} ions on the structure of model zinc fingers having either Cys_2His_2 or $Cys_2HisCys$ coordination motifs, as well as possible selectivity patterns.[49]

Overall, the results obtained so far showed that gold complexes are able to target zinc finger sites in vitro and revealed the influence of the different zinc coordination spheres (Cys_2His_2 vs $Cys_2HisCys$) in the formation of "gold fingers", with the domain of PARP-1 richer in Cys residues being the most reactive.

However, such a reaction deserves to be investigated in more detail in order to better characterize the species formed and the kinetics of the reaction and to assess the possible influence of biological thiols like glutathione (GSH) that may bind Au ions in cells.

Thus, here we characterize the reactivity of a $Zn(Cys)_4$ zinc finger model, $Zn{\cdot}L_{ZR}$, with a gold(III) complex, Auterpy ($[Au^{III}(terpy)Cl]^+$, where terpy = 2,2′,2″-terpyridine) via different techniques, including ultraviolet−visible (UV−vis) absorption, CD, X-ray absorption spectroscopy (XAS), high-performance liquid chromatography (HPLC) analysis, and mass spectrometry. Moreover, the influence of other thiol-containing molecules, such as GSH or β-mercaptoethanol (BME), on the reactivity of Auterpy with the zinc finger has been studied. Overall, we show that Auterpy can attack zinc fingers and substitute the Zn ion for Au^+ even in the presence of thiols.

RESULTS

Experimental Design. We have described previously zinc finger models using cyclic peptides with linear tails.[50,51] These peptides allow reproduction of the structure of various zinc finger sites with ca. 20−25 amino acids. In order to study the reactivity of zinc fingers with gold(III) complexes, we selected $Zn{\cdot}L_{ZR}$, a model for $Zn(Cys)_4$ zinc ribbon zinc fingers, for the following reasons: (i) the zinc ribbon fold is one of the most encountered zinc finger folds together with the treble clef fold;[29,31] (ii) this fold provides excellent shielding of the ZnS_4 core from the solvent compared to other zinc fingers.[52] Thus, it should constitute a benchmark for the reactivity of $Zn(Cys)_4$ zinc finger with gold(III) complexes. Figure 2A displays the sequence of peptide L_{ZR} and the solution structure of $Zn{\cdot}L_{ZR}$ as determined by NMR.[50] Concerning gold(III) complexes, we chose $[Au^{III}(terpy)(Cl)]Cl_2$[53] (Auterpy) as a prototype because the terpy ligand serves as an excellent probe for electronic absorption studies. Indeed, the absorption spectra of terpy and its gold(III) or zinc(II) complexes are very distinct (Figure 3A and Table 1). The terpy ligand displays a broad absorption at 290 nm,[54] whereas Auterpy shows several absorption bands between 300 and 400 nm with two maxima at 351 and 368 nm.[55] The terpy ligand forms 1:2 and 1:1 complexes with Zn^{2+},

DOI: 10.1021/acs.inorgchem.5b00360
Inorg. Chem. 2015, 54, 4104−4113

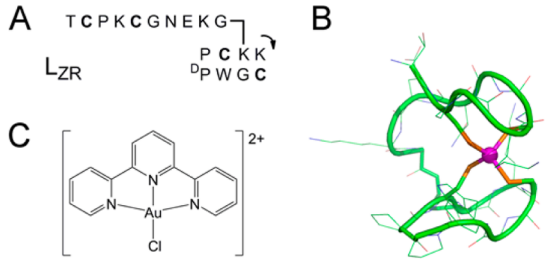

Figure 2. (A) Sequence of peptide L_{ZR}. (B) Solution structure of Zn·L_{ZR} (as determined by NMR at pH 6.3, 298 K).[50] (C) Auterpy complex.

as confirmed by the titration of terpy by Zn^{2+} (Figure 3B).[56,57] Upon the addition of Zn^{2+} to a solution of terpy, the band at 290 nm characteristic of a free terpy ligand decreases with a simultaneous increase of bands at 333 and 320 nm until 0.5 equiv of Zn^{2+} is added, which corresponds to formation of the 1:2 $[Zn^{II}(terpy)_2]^{2+}$ complex. After the addition of 0.5 equiv of Zn^{2+}, the 1:1 complex (most probably $[Zn(terpy)(H_2O)]^{2+}$) is progressively formed, with only slight changes observed in the spectrum: the bands at 320 and 333 nm shift to 319 and 329 nm, respectively, with isosbestic points at 331, 325, 318, and 308 nm. It is worth noting that the absorption maxima around 320 and 330 nm for both 1:2 and 1:1 zinc(II) complexes allow easy discrimination between free Au^{3+}- and Zn^{2+}-loaded terpy by UV−vis absorption and make this technique suitable to study the reaction between Zn·L_{ZR} and Auterpy. In addition, CD spectroscopy, mass spectrometry, and HPLC analyses were used to better characterize the behavior of the peptide. In a first set of experiments, the direct reaction between these two compounds was explored, and then the influence of free thiols such as GSH or BME, which mimics the cellular GSH, was investigated.

Characterization of the Direct Reaction between Auterpy and Zn·L_{ZR}. The reaction of Auterpy with Zn·L_{ZR} was first monitored by UV−vis absorption and CD spectroscopies. A total of 3 equiv of Auterpy was added to a solution of Zn·L_{ZR} (20 μM) in a phosphate buffer (20 mM, pH 7.0). The absorption spectrum recorded 2 h after mixing (Figure 4A) shows bands characteristic of the presence of Auterpy and $[Zn(terpy)_2]^{2+}$ complexes. Quantification of the former using the absorption at 367 nm indicates that 25 μM Auterpy remains

Table 1. Summary of the Absorption Bands of terpy, Auterpy, $[Zn^{II}(terpy)_2]^{2+}$, and $[Zn^{II}(terpy)(H_2O)]^{2+}$ in a Phosphate Buffer (20 mM, pH 7.0) at 298 K

	λ, nm (ε, M^{-1} cm^{-1})
terpy	290 (15800)
Auterpy	367 (11300), 351 (11100), 335 (8600), 292 (15400), 283 (16700), 274 (16900)
$[Zn^{II}(terpy)_2]^{2+}$	333 (35700), 320 (34100), 282 (25400), 275 (22300), 265 (19100)
$[Zn^{II}(terpy)(H_2O)]^{2+}$	329 (16200), 319 (16100), 282 (15600), 275 (11900)

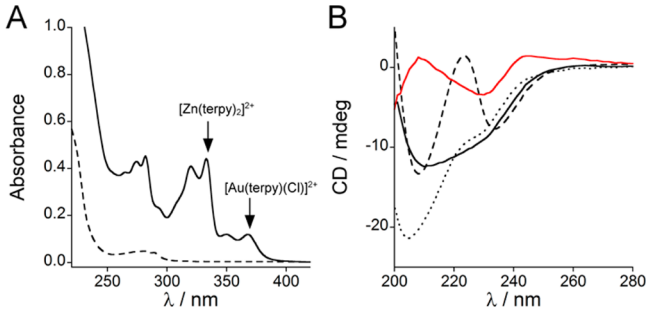

Figure 4. (A) UV−vis absorption and (B) CD spectra of a solution of Zn·L_{ZR} (20 μM) in a phosphate buffer (20 mM, pH 7.0) before (black dashed line) and after (black solid line) the addition of Auterpy (3 equiv , 60 μM) (path length = 0.4 cm). In part B is also shown the CD spectrum of L_{ZR} (dotted line) and the CD spectrum recorded after the reaction of Auterpy (60 μM) with a solution of Zn·L_{ZR} (20 μM) in a phosphate buffer (20 mM, pH 7.0) containing BME (1 mM) (red solid line).

in solution and thus that ca. 2 equiv of Auterpy has been consumed in the reaction with Zn·L_{ZR}. In agreement, quantification of $[Zn(terpy)_2]^{2+}$ by the absorption at 333 nm (taking into account the absorption of the remaining Au^{III} complex at this wavelength) confirms the release of 20 μM Zn^{2+} by reaction between the zinc finger peptide and the gold(III) complex. Figure 4B shows the CD spectrum of the same solution, together with those of Zn·L_{ZR} and free L_{ZR} (reduced form). The differences in the CD spectra clearly demonstrate that the zinc finger fold has been altered and that a new species different from the free L_{ZR} has been formed.

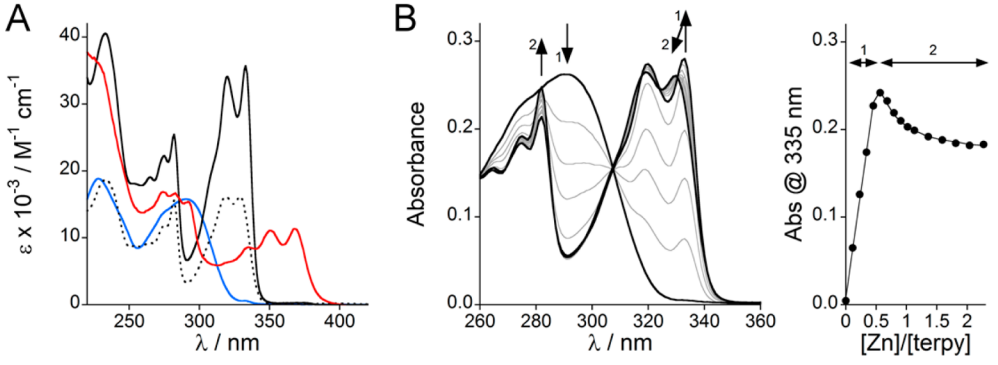

Figure 3. (A) Absorption spectra of terpy (blue line), Auterpy (red line), $[Zn^{II}(terpy)_2]^{2+}$ (black solid line), and $[Zn^{II}(terpy)(H_2O)]^{2+}$ (black dotted line) in a phosphate buffer (20 mM, pH 7.0) at 298 K. (B) Titration of terpy (17 μM) by Zn^{2+} in a phosphate buffer (20 mM, pH 7.0) at 298 K. The graph on the right shows the evolution of the absorbance at 335 nm together with the fit (solid line) obtained using the program *SPECFIT*,[58] taking into account 1:2 and 1:1 Zn/terpy complexes. The fit yielded log $K_{1:1}$ = 7.8(3) and log $K_{1:2}$ = 14.3(3), where $K_{1:1}$ and $K_{1:2}$ are the apparent association constants for 1:1 and 1:2 complexes. All spectra were corrected for dilution.

DOI: 10.1021/acs.inorgchem.5b00360
Inorg. Chem. 2015, 54, 4104−4113

The reaction was investigated further, and the kinetics of the reaction was evaluated. For this purpose, 0.22 equiv of Zn·L_{ZR} was added to a 30 μM solution of Auterpy in a phosphate buffer (pH 7.0), leading to ca. 25% reduction of the gold compound's absorbance at 367 nm during the mixing time (Figure 5), which

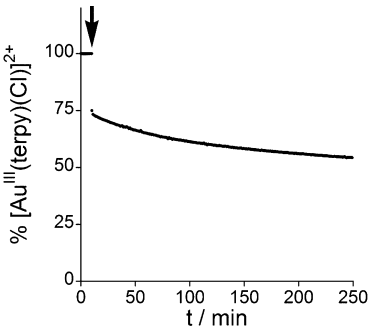

Figure 5. Time dependence of the consumption of Auterpy after the addition of Zn·L_{ZR} (6.6 μM) to Auterpy (30 μM) in a phosphate buffer (20 mM, pH 7.0). The concentration of Auterpy is monitored by changes in the absorption at 367 nm against time (path length = 1 cm). The arrow indicates the time of the addition of the zinc complex.

indicates the immediate consumption of 25% of the gold(III) complex. Then, the absorbance slowly decreases and tends to ca. 45% of the initial absorbance after overnight incubation. This shows that two successive reactions (at least) take place at very different time scales (seconds vs hours).

In order to identify the product formed during the first kinetic phase, we performed a "fast" titration without any delay between the addition of Zn·L_{ZR} and the recording of the spectrum (spectra were recorded ca. every 2 min). Figure 6A displays the evolution of the UV–vis spectra. It shows the disappearance of Auterpy (367 nm) and the appearance of zinc terpyridine complexes (330 nm), with an end point for the titration when ca. 1.0 equiv of Zn·L_{ZR} was added.

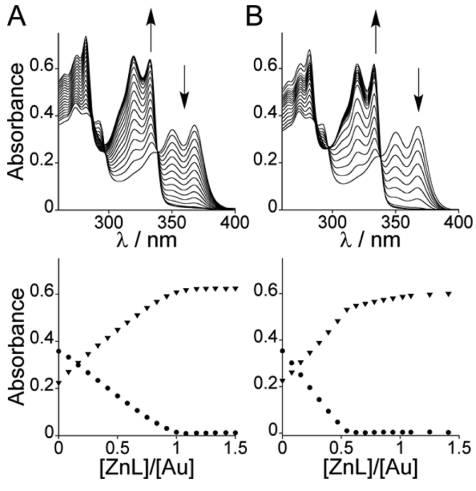

Figure 6. (A) "Fast" UV–vis titration of Auterpy (32 μM) by Zn·L_{ZR} in a phosphate buffer (20 mM, pH 7.0). The titration was performed without any delay between the addition of Zn·L_{ZR} and the recording of the spectrum. (B) "Slow" titration of Auterpy (32 μM) by Zn·L_{ZR} performed as in part A but waiting 1 h between the addition of Zn·L_{ZR} and the recording of the spectrum. The bottom panels show the absorbance at 367 nm (dots) and 331 nm (triangles) versus Zn·L_{ZR} equivalents. All spectra were corrected for dilution.

The positive-mode ESI-MS spectrum of the reaction mixture near the end point shows peaks at m/z 265.1 (2+) and 332.1 (+), which correspond to $[Zn(terpy)_2]^{2+}$ and $[Zn(terpy)(Cl)]^{+}$, respectively, confirming zinc release from the peptide. No other peaks could be detected. In negative mode, besides unreacted Zn·L_{ZR}, a peak at m/z 1075.3 (2–) was observed (Figure 7A) corresponding to a $[M - H]^{2-}$ ion with M =

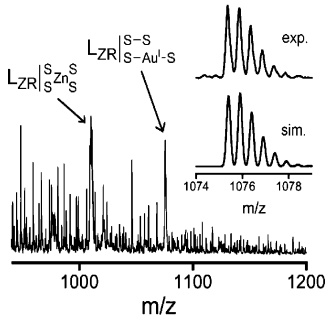

Figure 7. ESI-MS spectrum (negative mode) of the solution at the end point of the "fast" titration of Auterpy (32 μM) by Zn·L_{ZR}. The experimental and simulated zoom scans of the peak at m/z 1075.3 (2–) corresponding to $[M - H]^{2-}$ with M = L_{ZR}(S–S,S–Au–S) = $[C_{83}H_{126}N_{24}O_{23}S_4Au]^{-}$ are shown.

$[C_{83}H_{126}N_{24}O_{23}S_4Au]^{-}$. Because the formula of L_{ZR} is $C_{83}H_{130}N_{24}O_{23}S_4$, this peak is associated with a species that has lost four protons and bound a Au ion, and two possibilities can be considered. The most likely is the complex L_{ZR}(S–S,S–Au^{I}–S), which contains one disulfide and a Au^{I} ion bound to two thiolates: the linear geometry is common for (di)-thiolategold(I) complexes[3,59] and has already been observed in proteins.[60] The alternate Au^{III}·L_{ZR} complex, which has its four cysteine thiolates bound to the Au^{III} ion, appears unlikely based on the following considerations: (i) Homoleptic $Au^{III}(SR)_4$ complexes are rare. They were reported in the case of electron-deficient thiolates only (e.g., R = C_6F_5). They can be stabilized in the solid state but are very unstable in solution. They decompose into oligomeric gold(I) thiolate complexes and disulfides.[61,62] (ii) Homoleptic $Au^{III}(SR)_4$ complexes display an intense red color because of ligand-to-metal charge-transfer transitions between the thiolate ligands and the Au^{III} ion that were not observed during our titration.[61,62] (iii) Auterpy has a high redox potential in aqueous solution (+0.62 V/NHE[55]) which makes it a good oxidizer for free thiols (the RSSR/RSH couple is in the range −0.3 to −0.2 V/NHE.[63] Of course, zinc binding will decrease cysteine oxidizability but probably not enough to compensate for the ca. 1 V difference in the redox potentials.

In order to determine the nature of the gold peptide complex, XAS was used. For this purpose, Zn·L_{ZR} (1.6 mM) was reacted with Auterpy (0.8 mM) in a phosphate buffer containing 20% glycerol. Auterpy and aurothiomalate (Figure 1) samples were also prepared for comparison purposes. XAS spectra of the frozen solution were recorded at liquid-helium temperature. The normalized Au edge X-ray absorption near-edge structure (XANES) spectra are displayed in Figure 8A. XANES is sensitive to the valence and to the site geometry of the probed atom. The spectrum of the sample corresponding to the reaction of Zn·L_{ZR} with Auterpy (c) is clearly different from that of Auterpy (a) and strikingly similar to that of aurothiomalate (b), suggesting the formation of a S–Au^{I}–S entity. This was confirmed by fitting of the extended X-ray

DOI: 10.1021/acs.inorgchem.5b00360
Inorg. Chem. 2015, 54, 4104–4113

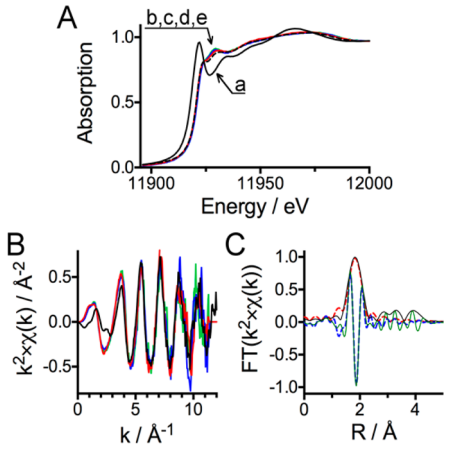

Figure 8. (A) Normalized Au edge XANES spectra of solutions of the reference compounds Auterpy (a, black solid line) and aurothiomalate (b, black dashed line) and solutions c (red), d (blue), and e (green) prepared by reacting Zn·L_{ZR} (1.6 mM) with 0.5 equiv of Auterpy (c), Zn·L_{ZR} (500 μM) in BME (55 mM) with 1.0 equiv of Auterpy (d), and Zn·L_{ZR} (250 μM) in BME (55 mM) with 2.0 equiv of Auterpy (e). (B) k^2-weighted EXAFS spectra of aurothiomalate (black) and solutions c (red), d (blue), and e (green). (C) Fourier transform of the k^2-weighted EXAFS spectra of solution b: the experimental and fitted moduli are shown in black and blue, respectively, and the experimental and fitted imaginary parts are shown in red and green, respectively.

absorption fine structure (EXAFS) data (Figure 8B,C). EXAFS is sensitive to the nature, number, and distance of the neighbors around the central atom. Fitting was done with two S atoms around Au, with a Au−S distance of 2.27(2) Å in good agreement with those of aurothiomalate determined by XAS[64,65] or X-ray diffraction[59] (Table 2). XAS measurements

Table 2. EXAFS Fitting Results for Aurothiomalate and Solutions c−e (See the Legend of Figure 8)

	Au−S distance, Å	σ^2	no. of Au nearest neighbors (S)
aurothiomalate	2.29 ± 0.01	0.0016	2
Zn·L_{ZR} + 0.5 equiv of Auterpy (c)	2.27 ± 0.02	0.0017	2
Zn·L_{ZR} + BME + 1 equiv of Auterpy (d)	2.29 ± 0.01	0.0006	2
Zn·L_{ZR} + BME + 2 equiv of Auterpy (e)	2.27 ± 0.01	0.003	2

thus confirm that L_{ZR}(S−S,S−Au^{I}−S) is formed and not Au^{III}·L_{ZR}. Therefore, Auterpy oxidizes two zinc-bound thiolates into a disulfide, and the reduced Au ion becomes coordinated by the two remaining thiolates.

When a "slow" titration is performed (Figure 6B), allowing the second kinetic phase to proceed (spectra were recorded ca. every 1 h), the end point of the titration is observed at ca. 0.5 equiv of Zn·L_{ZR}. The ESI-MS spectrum at the end point shows peaks at m/z 978.3 (2+), 989.3 (2+), and 1955.8 (+) corresponding to the bis(disulfide) peptide L_{ZR}(S−S,S−S) (M = $C_{83}H_{126}N_{24}O_{23}S_4$; calculated m/z 978.41 for $[M + 2H]^{2+}$, 989.41 for $[M + Na + H]^{2+}$, and 1955.84 for $[M + H]^{+}$). Therefore, the slow kinetic phase is assigned to oxidation of the S−Au^{I}−S moiety of L_{ZR}(S−S,S−Au^{I}−S) into a disulfide by Auterpy. The formation of the bis(disulfide) products L_{ZR}(S−S,S−S) was confirmed by HPLC monitoring. Parts A and B of Figure 9 display the chromatograms of L_{TC} (reduced form,

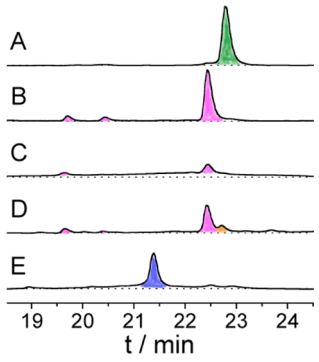

Figure 9. Analytical HPLC chromatograms of (A) Zn·L_{ZR} (20 μM), (B) the three bis(disulfide) isomers of L_{ZR}(S−S,S−S) obtained by oxidation of Zn·L_{ZR} (20 μM) by H_2O_2 (10 mM), and (C−E) the crude mixture of the reaction of Zn·L_{ZR} (20 μM) with Auterpy (60 μM). Parts C and D were obtained without (C) and with (D) the addition of thiourea (50 mM) prior to injection, and part E was obtained when the reaction was performed in the presence of BME (1 mM).

green peak at t_R = 23.0 min) and the three isomers of L_{ZR}(S−S,S−S) (pink peaks at t_R = 19.7, 20.4, and 22.4 min) obtained by H_2O_2 oxidation of Zn·L_{ZR}, respectively. Figure 9C shows the chromatogram obtained by mixing Zn·L_{ZR} with 3.0 equiv of Auterpy. Two small peaks corresponding to two out of the three bis(disulfide) peptides were observed over a very broad peak that extends from 18 to 25 min. This broad peak was all the more intense compared to those of L_{ZR}(S−S,S−S) as Auterpy was in excess. Under suspicion that adventitious binding of Au ions to the peptides was responsible for this, thiourea (50 mM) was added to the sample prior to the HPLC injection to bind the excess of gold salt and thin peaks were recovered (Figure 9D), confirming the disappearance of reduced L_{ZR} and the presence of the three isomers of the bis(disulfide) peptides L_{ZR}(S−S,S−S). Several other small peaks were observed in addition to those corresponding to the three bis(disulfides). Only the peak eluting at t_R = 22.7 min (orange) was accumulated in sufficient amount to be collected and analyzed by ESI-MS. A mass peak at m/z 994.4 (2+) was observed that corresponded to a +32 mass increase compared to the bis(disulfide) product (calculated m/z 994.41 for $[M + 2H]^{2+}$ with $C_{83}H_{126}N_{24}O_{25}S_4$). The formation of thiosulfinate in a zinc finger has already been reported.[66] This suggests possible overoxidation of the disulfides into two thiosulfinates [RS(O)−SR] or one thiosulfonate ester [$RS(O)_2$−SR] by excess Auterpy.[67,68] The same amount of overoxidized peptide was observed when the reaction was performed under air or inert atmosphere (glovebox), showing that it was not due to O_2. This species was not detected by ESI-MS analyses of a crude mixture of Zn·L_{ZR} and Auterpy, and its formation was not investigated further.

In order to get deeper insight into the kinetics of the first step, which yields L_{ZR}(S−S,S−Au^{I}−S), we monitored the decrease of absorbance at 367 nm of Auterpy (1.5 μM) using a stopped-flow apparatus in conditions of excess Zn·L_{ZR} (28−86 μM). Each kinetic trace (Figure 10) could be nicely fit to a monoexponential decay, which yields an apparent first-order rate constant k^{obs} that is proportional to the concentration of Zn·L_{ZR} (Figure 10). Therefore, the first step follows a second-order kinetic law $r = k$[Zn·L_{ZR}][Auterpy] with a rate constant k = (3.3 ± 0.3) × 10^5 M^{-1} s^{-1}. Hence, at the micromolar

DOI: 10.1021/acs.inorgchem.5b00360
Inorg. Chem. 2015, 54, 4104−4113

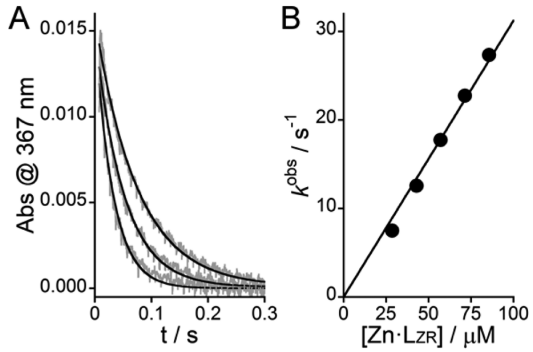

Figure 10. (A) Stopped-flow absorbance monitoring (λ = 367 nm) of the reaction of Auterpy with Zn·L_{ZR}. The kinetic traces displayed in gray were recorded for 1.5 μM Auterpy and 42.9, 57.1, and 85.7 μM Zn·L_{ZR} in a phosphate buffer (20 mM, pH 7.0, 298 K). The solid lines correspond to monoexponential fits. (B) Plot of the apparent first-order rate constant k^{obs} derived from monoexponential fits against the concentration of Zn·L_{ZR}. The slope yields the second-order rate constant $k = (3.3 \pm 0.3) \times 10^5$ M^{-1} s^{-1}.

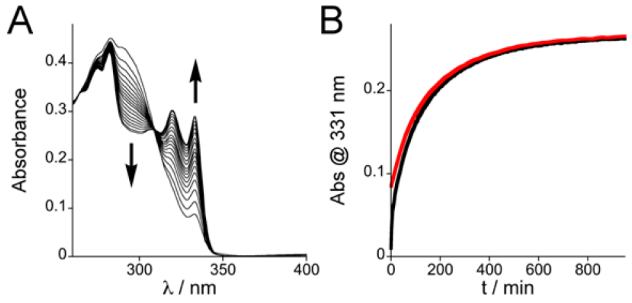

Figure 11. Absorbance monitoring of the reaction between Auterpy and Zn·L_{ZR} in the presence of GSH. (A) Evolution of the absorption spectra recorded after the addition of Auterpy (70 μM) to a solution containing Zn·L_{ZR} (20 μM) and GSH (1 mM) in a phosphate buffer (20 mM, pH 7.0). (B) Evolution of the absorbance at 331 nm against time (red) when Auterpy is added after the mixing of Zn·L_{ZR} (20 μM) and GSH (1 mM) and (black) when Zn·L_{ZR} (20 μM) is added to the solution after the mixing of Auterpy (70 μM) and GSH (1 mM).

concentrations investigated, the time scale for the first and second steps fall in the second and hour ranges, respectively.

Influence of Free Thiols. The GSH concentration in cells is buffered in the millimolar range, thereby providing a reducing environment.[69] Disulfide-containing products L_{ZR}(S−S,S−Au−S) and L_{ZR}(S−S,S−S) formed by the direct reaction of Auterpy with Zn·L_{ZR} should not be stable in the presence of a millimolar concentration of GSH. In addition, gold(III) complexes can be reduced by an excess of thiol to yield gold(I) thiolate complexes, which are oligomeric entities of the formula $(RS-Au^{I})_n$.[3,70,71] Therefore, in cells, these reactions may interfere with the reaction between gold(III) complexes and zinc fingers. When Auterpy (60 μM) is reacted with GSH or BME (1 mM), the absorption at 367 nm vanishes in a few seconds during the mixing time, with concomitant appearance of a broad absorbance at 290 nm characteristic of the free terpy ligand, suggesting reduction of the Auterpy complex and, consequently, the formation of gold(I) thiolate species. Recently, the kinetics of the reaction of Auterpy with GSH at pH 7.0 has been reported, and the first step is ca. 100-fold slower than that measured for Zn·L_{ZR}.[72] Therefore, a millimolar amount of free thiol should be able to compete with Zn·L_{ZR} in the 10 μM concentration range for reaction with Auterpy. Hence, the reaction between Auterpy and Zn·L_{ZR} was investigated in the presence of 1 mM GSH or BME. As a preliminary study, we checked by CD spectroscopy that neither GSH (1 mM), BME (1 mM), nor terpyridine (100 μM) was able to alter the zinc finger and displace Zn^{2+} from Zn·L_{ZR}. Then, 3.5 equiv of Auterpy was added to a solution of Zn·L_{ZR} (20 μM) in a phosphate buffer (20 mM, pH 7.0) containing GSH (1 mM). Figure 11A displays the evolution of the absorption spectra recorded over 16 h. The first spectrum recorded 30 s after the addition of the gold(III) complex shows absorption bands of both free terpyridine and $[Zn^{II}(terpy)_2]^{2+}$ at 290 and 331 nm, respectively, with the concentration of $[Zn^{II}(terpy)_2]^{2+}$ being ca. 7 μM. No absorption at 367 nm is observed, indicating that the gold(III) complex has reacted completely within the first seconds (Figure 11B). Then, the band at 331 nm increases slowly and plateaus after ca. 12 h with a concomitant decrease of the band at 290 nm. At the end of the reaction, the concentration of $[Zn^{II}(terpy)_2]^{2+}$ is ca. 19 μM, based on the extinction coefficient given in Table 1. This means that Zn^{2+} has been fully released from the peptide. In another experiment, Auterpy (70 μM) was reacted with GSH (1 mM) in order to form GS−Au^{I} species, and then Zn·L_{ZR} (20 μM) was added. A very similar behavior was observed regarding the evolution of the spectrum and the time scale (Figure 11B). The only difference is that almost no $[Zn^{II}(terpy)_2]^{2+}$ is detectable in the first spectrum recorded ca. 5−10 s after the addition of Zn·L_{ZR} compared with ca. 7 μM when Auterpy is added to the Zn·L_{ZR}/GSH mixture. This shows that gold(I) thiolate species are able to displace Zn^{2+} from Zn·L_{ZR}. The fact that the amount of $[Zn(terpy)_2]^{2+}$ formed in the first seconds during mixing depends on the order of the addition of reactants confirms that GSH can kinetically compete with Zn·L_{ZR} for reaction with Auterpy. Replacing GSH with BME yields a similar but faster reaction (ca. 1 h vs 12 h to complete the reaction).

In order to identify the products formed in the presence of thiols, 3 equiv of Auterpy was added to a solution of Zn·L_{ZR} (20 μM) and BME (1 mM) in a phosphate buffer (20 mM, pH 7.0), and the resulting solution was analyzed by HPLC, CD, and ESI-MS after 1 h. Additionally, two similar samples, but at higher concentration, were prepared for XAS analysis with 1 and 2 equiv of Auterpy versus Zn·L_{ZR} (250 μM) in the presence of BME (55 mM). XANES and EXAFS spectra (Figure 8A,B and Table 2) unambiguously establish the formation of S−Au^{I}−S species. The HPLC chromatogram (Figure 9E) shows the disappearance of L_{ZR} (reduced form) and the appearance of a new major species at t_R = 21.3 min (colored in blue). The CD spectrum (Figure 4B, red spectrum) is different from that obtained by the direct reaction between Zn·L_{ZR} and Auterpy, confirming the presence of a new species. On the ESI-MS spectrum displayed in Figure 12, Zn·L_{ZR} is hardly detectable at m/z 1011.3 (2+), and the major peak at m/z 1176.3 (2+) can be assigned to the complex L_{ZR}(S−Au^{I}−S,S−Au^{I}−S) with two Au^{+} ions bound to the four cysteinates (calculated m/z 1176.40 for $[M + 4H]^{2+}$ with M = L_{ZR}(S−Au−S,S−Au−S) = $[C_{83}H_{126}N_{24}O_{23}S_4Au_2]^{2-}$) and its Na^{+} and K^{+} adducts. A smaller peak at m/z 1077.3 (2+) corresponds to the complex L_{ZR}(S−S,S−Au^{I}−S) with probably two cysteines engaged in a disulfide and the two others bound to a Au^{+} ion (calculated m/z 1077.41 for $[M + 3H]^{2+}$ with M = L_{ZR}(S−S,S−Au−S) = $[C_{83}H_{126}N_{24}O_{23}S_4Au]^{-}$). No peak corresponded to free reduced L_{ZR} or to the bis(disulfide) peptide.

DOI: 10.1021/acs.inorgchem.5b00360
Inorg. Chem. 2015, 54, 4104−4113

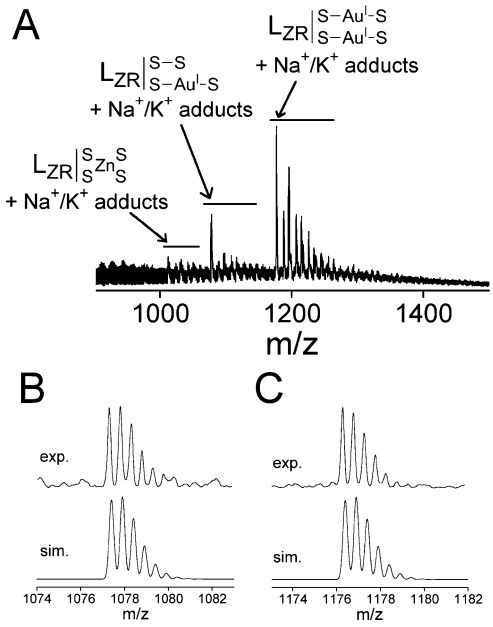

Figure 12. ESI-MS analysis of the reaction of Zn·L_{ZR} (20 μM) and BME (1 mM) with $Au^{III}(terpy)(Cl)]^{2+}$ (70 μM) in an ammonium acetate buffer (20 mM, pH 7.0). (A) Region at m/z 900−1500 (positive mode) of the ESI-MS spectrum. (B and C) Experimental zoom scans of the peaks at m/z 1077.3 (2+) and 1176.3 (2+) corresponding to species $[M + 3H]^{2+}$ with M = L_{ZR}(S−S,S−Au^I−S) = $[C_{83}H_{126}N_{24}O_{23}S_4Au]^-$ and $[M + 4H]^{2+}$ with M = L_{ZR}(S−Au^I−S,S−Au^I−S) = $[C_{83}H_{126}N_{24}O_{23}S_4Au_2]^{2-}$, respectively.

DISCUSSION

Zinc Ribbon Zinc Fingers Can Be Readily Destroyed by Direct Reaction with Redox-Active Gold(III) Complexes. The present study shows that the reaction of Auterpy with Zn·L_{ZR}, a $Zn(Cys)_4$ zinc finger with a zinc ribbon fold, leads to the release of Zn^{2+} from the peptide and the formation of a gold peptide complex, where two cysteines have been oxidized into a disulfide and the two remaining cysteines are bound to the reduced Au^+ ion (Scheme 1). This reaction is very fast, with the rate constant of the rate-determining step being k = (3.3 ± 0.3) × 10^5 M^{-1} s^{-1}. It prevails over the simple substitution of Zn^{2+} for Au^{3+} because no spectroscopic evidence of the complex Au^{III}·L_{ZR} has been observed.[61] This is supported by calculations indicating that the reduction of Au^{III} to Au^I by alkylthiolates is favored over the ligand-exchange reaction.[71] In conditions of excess Auterpy, a second oxidation occurs at a much longer time scale than the formation of the first disulfide (hours vs seconds in the concentration range investigated) to give the bis(disulfide) peptide (Scheme 1). The latter can be further oxidized into thiosulfinate or thiosulfonate esters. It is worth noting that all of these products should have a fold different from that of the native zinc finger (see the CD spectra in Figure 4B) with the loss of the protein structure and activity as a consequence. The behavior observed with our $Zn(Cys)_4$ zinc finger model is in agreement with the removal of Zn^{2+} from $Cys_2HisCys$ zinc finger sites from the HIV nucleocapsid by gold(III) complexes that has been reported previously,[47] based on mass spectrometry measurements. However, the latter study relied on the observation of both oxidized peptides and gold peptide adducts with the loss of zinc protein adducts without quantification that would have revealed the stoichiometry of the reaction and the precise oxidation state of the Au ions bound to the protein. In the case of the reaction of the zinc finger of PARP-1 with an excess of the gold(III) complex auphen, binding of a Au^{III} ion to the peptide was established by HRMS.[48] Similarly, auphen was shown to form gold(III) adducts with a Cys_2His_2 model peptide by mass spectrometry.[49] In general, reactions of gold(III) compounds with zinc finger proteins show a higher reactivity with the $Cys_2HisCys$ zinc finger than with Cys_2His_2, likely due to the presence of fewer aurophilic cysteines in the latter.[49,73] Within this frame, the present study supports the fact that Cys_4 zinc finger sites, at least those with a zinc ribbon fold, are susceptible to attack by gold(III) complexes such as Auterpy but that Au^{III} ions have the tendency to be reduced upon binding to the highly aurophilic Cys_4 domains. Interestingly, the nature of the species formed may differ between zinc finger domains depending on the type of coordination sphere of the zinc finger (Cys_4, $Cys_2HisCys$, and Cys_2His_2), on the fold of the zinc finger, and on the presence in a sequence of amino acids able to coordinate Au^+ or Au^{3+}. Thus, further studies are necessary, using other zinc fingers, to gain deeper insight into these systems. Comparisons between zinc fingers of various classes[28−31,39] should help to determine the factors that govern the reactivity between zinc fingers and gold complexes.

Scheme 1. Destruction of the $Zn(Cys)_4$ Zinc Ribbon Zinc Finger Model Zn·L_{ZR} by Direct Reaction with Auterpy

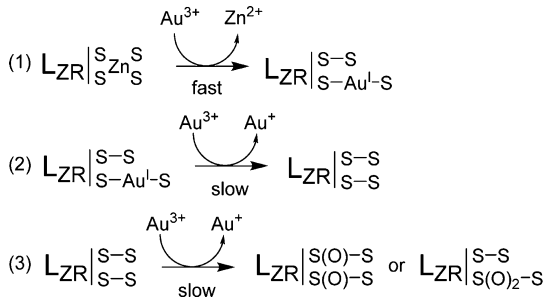

Are Gold(I) Species the Real Damaging Agent for Zinc Fingers in Cells? Although in vitro direct reaction of gold(III) with zinc finger is efficient, in cells, zinc fingers have to compete with free thiols for gold(III) complexes. The reaction of Auterpy with Zn·L_{ZR} in the presence of GSH or BME leads to a peptide with S−Au^I−S motifs at a reasonable time scale (hours at the concentrations investigated). Although the direct reaction of Auterpy with Zn·L_{ZR} is still possible (at least partly) in the presence of excess thiols based on kinetics, the present study shows that indirect reaction, where (i) the gold(III) complex is first reduced to gold(I) thiolates and (ii) metal exchange occurs between gold(I) thiolates and the zinc finger protein, is also possible (Scheme 2, pathway A). The direct reaction yields a peptide with one or two disulfides that will be reduced by GSH, making cysteines available for binding of Au^+ generated by the reaction of excess gold(III) complex with thiols (pathway B). Therefore, both pathways give the same product, where Zn^{2+} is replaced by Au^+ ions, which may be detrimental to the protein fold and function.

Indeed, the results described above for the reaction between Zn·L_{ZR} and Auterpy in the presence of excess thiols suggest that gold complexes can damage zinc fingers in cells that contain a millimolar concentration of GSH. This reinforces the idea that important zinc finger proteins like PARP-1 may be inhibited by gold complexes in vivo.[48,74] Moreover, if Au^I is able to displace Zn^{2+} from zinc finger proteins and form S−Au^I−S

DOI: 10.1021/acs.inorgchem.5b00360
Inorg. Chem. 2015, 54, 4104−4113

Scheme 2. Destruction of the $Zn(Cys)_4$ Zinc Finger Model $Zn{\cdot}L_{ZR}$ by Auterpy in the Presence of Free Thiols

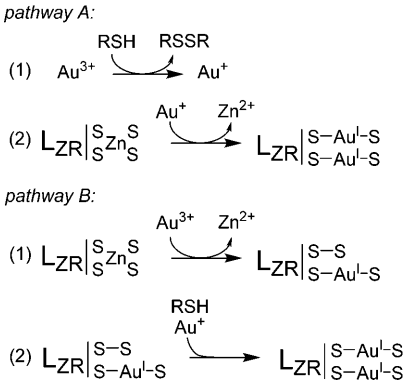

entities, it should also be able to bind to other proteins having pairs of free cysteines.

CONCLUSION

In this Article, we have described the reactivity of Auterpy, a redox-active gold(III) complex, with $Zn{\cdot}L_{ZR}$, a $Zn(Cys)_4$ zinc finger model of the zinc ribbon class, both in the absence and in the presence of free thiols mimicking GSH in cells. We have shown that direct reaction between the gold(III) complex and $Zn{\cdot}L_{ZR}$ is fast, leading to a reduction of Au^{3+} to Au^{+}, which binds to two cysteines of the zinc finger, and formation of a disulfide. As a consequence, Zn^{2+} is expelled from the peptide, and formation of a "gold finger" domain is achieved. Further oxidation reactions can proceed, but slower, in the presence of excess gold(III) complex. Free thiols such as GSH and BME have a strong impact on this reaction because they compete with $Zn{\cdot}L_{ZR}$ to form Au^{+} species and they are also able to reduce disulfides. Moreover, the zinc finger is still damaged in the presence of free thiols, with Zn^{2+} being replaced by two Au^{+} ions.

To determine the species induced by the substitution of Zn^{2+} with Au ions in zinc fingers and to correlate them to possible inhibition properties are fundamental to the understanding of the mechanism of action of gold-based cytotoxic agents at a molecular level. In fact, our findings support the idea that zinc finger proteins may constitute realistic pharmacological targets for this promising class of metal compounds.

Finally, regarding the possible use of redox-active gold(III) coordination complexes as anticancer agents, they can be considered as pro-drugs generating gold(I) thiolate and free ligand in cells, both capable of being toxic acting on very different targets. The richer coordination chemistry of gold(III) compared to gold(I) allows the design of complexes with enhanced chemical diversity, and thus it offers numerous possibilities to tune the reactivity of the resulting gold compounds by modulating cell targeting and uptake properties.

EXPERIMENTAL SECTION

Materials and Methods. *N*-α-Fmoc-protected amino acids, coupling reagent, and resin for peptide synthesis were obtained from Novabiochem. Other reagents, solvents, buffers, and metal salts were purchased from Sigma-Aldrich. $[Au^{III}(terpy)(Cl)]Cl_2$ (Auterpy) was synthesized according to work by Hollis and Lippard.[53] HPLC analyses and purifications were performed on a VWR LaPrep system. Analytical HPLC (PurospherStar RP18e 5 μm C18 particle, 150 mm × 4.6 mm, gradient 5−50% B in 28 min) was performed at 1.0 mL min^{-1} with UV monitoring at 214 nm. ESI-MS analyses were performed on a Thermo LXQ spectrometer. UV−vis spectra were recorded on a PerkinElmer Lambda 35 spectrophotometer or on a Varian Cary 50 spectrophotometer. CD spectra were recorded on an Applied Photophysics Chirascan spectropolarimeter or on a Bio-Logic MOS-450 AF-CD spectropolarimeter. Stopped-flow kinetic measurements were performed using a Bio-Logic SFM-400 stopped-flow device coupled to a MOS-450 AF-CD spectrometer. All spectrometers were equipped with a thermoregulated cell holder. All buffer or metal solutions were prepared with Milli-Q water (Millipore) and purged with argon. Buffer solutions were treated with Chelex 100 resin (Biorad) to remove metal traces. A $ZnCl_2$ (99.999%) stock solution was prepared by dissolving the metal salt in water.

Preparation of Stock Solutions. Auterpy stock solutions were prepared by dissolving $[Au^{III}(terpy)Cl]Cl_2$[53] in water. The concentration was determined using the absorbance at 367 nm ($\varepsilon = 1.1 \times 10^4$ M^{-1} cm^{-1}).[55] The Auterpy stock solution could be stored at −20 °C for several days. For a $Zn{\cdot}L_{ZR}$ stock solution, L_{ZR} was dissolved in water under an argon atmosphere. Its concentration was determined by measuring the cysteine-free thiol concentration using Ellman's reagent[75] and checked by Zn^{2+} titration. Then, the peptide was diluted to the desired concentration in a phosphate buffer (20 mM, pH 7.0) under an argon atmosphere, and 1.0 equiv of a $ZnCl_2$ solution in water was added. BME and GSH stock solutions were prepared by diluting or dissolving the thiol in a phosphate buffer (20 mM, pH 7.0). Their concentrations were determined using Ellman's reagent.[75]

UV−Vis Absorption and CD Measurements. Samples for UV−vis absorption and CD spectra were prepared in a rubber-sealed quartz cell (1 or 0.4 cm path length) under argon. UV−vis absorption was recorded at 298 K in the 200−500 nm range every 1 nm at a scan rate of 480 nm min^{-1}. The CD signal was recorded at 298 K in the 200−350 nm range every 1 nm with 2 s signal averaging for each point. Each spectrum was recorded two times and averaged. Spectra were corrected for dilution.

Stopped-Flow Measurements. The kinetics of the reaction of Auterpy with $Zn{\cdot}L_{ZR}$ was monitored following the absorbance of Auterpy at 367 nm. Solutions of the gold salt and of the zinc complex were mixed using a Biologic stopped-flow apparatus. After mixing, the initial concentration of Auterpy was 1.5 μM and the zinc complex was always kept in large excess (>15 equiv). Kinetic traces were fitted with a single exponential to yield the observed first-order rate constant k^{obs}.

XAS. Solutions containing 20% glycerol were prepared in a glovebox, frozen in a 50 μL sample holder, and placed in a helium cryostat for measurements. XAS measurements were carried out at the ESRF (Grenoble, France), which was operating with a ring current of 90 mA. Spectra were collected at the BM30B (FAME) beamline using a Si(220) double-crystal monochromator with dynamic sagittal focusing and two parabolic rhodium-coated mirrors for harmonic rejection. The spot size was full width at half-maximum of 300 μm horizontal × 100 μm vertical.[76] The incoming photon energy was calibrated with a gold metallic foil, by defining the first inflection point of its XAFS spectrum at 11.919 keV. The samples were frozen at liquid-helium temperature in order to avoid X-ray beam damage during data collection. The spectra were collected in fluorescence mode with a 30-element solid-state germanium detector (Canberra). A total of 10 scans of 40 min each were averaged to obtain the spectrum of each sample. Data from each detector channel were inspected for glitches or dropouts before inclusion in the final average.

Data analysis was performed using the *Horae* package,[77] including *ATHENA* for data extraction and *ARTEMIS* for shell fitting. XANES spectra were background-corrected by a linear regression through the preedge region and a low-order polynomial curve through the postedge region and normalized to the edge jump. For extraction of the EXAFS part, E_0 was defined at the maximum of the first derivative of the spectrum. A cubic spline was fitted through the EXAFS energy range and subtracted to remove the background. The k^2-weighted EXAFS spectra were Fourier-transformed over the k range of 3.25−10 $Å^{-1}$ (3.17−11.6 $Å^{-1}$ for aurothiomalate) using a Hanning window. Fits were performed on the Fourier-transformed spectra over the R range of 1−2.6 Å. Quick first-shell theory was used to create the structural

DOI: 10.1021/acs.inorgchem.5b00360
Inorg. Chem. 2015, 54, 4104−4113

model: 2 S atoms at 2.3 Å from the absorbing Au atom. The amplitude reduction factor S_0^2 was set to 0.84, as found on the gold metal foil.

AUTHOR INFORMATION

Corresponding Authors

*E-mail: jean-marc.latour@cea.fr.
*E-mail: olivier.seneque@cea.fr.

Notes

The authors declare no competing financial interest.

ACKNOWLEDGMENTS

Funding for this project was provided by the Région Rhône-Alpes (CIBLE 10 015762, doctoral fellowship for A.J.). J.-M.L. and O.S. also acknowledge the partial support of Labex ARCANE (ANR-11-LABX-0003-01). A.C. thanks the University of Groningen (Rosalind Franklin Fellowship) for financial support. Members of the European COST Action CM1105 are gratefully acknowledged for stimulating discussions. The French CRG Committee is acknowledged for a provision of synchrotron radiation beamtime.

REFERENCES

(1) Smolen, J. S.; Steiner, G. *Nat. Rev. Drug Discovery* **2003**, *2*, 473.
(2) Berners-Price, S. J.; Filipovska, A. *Metallomics* **2011**, *3*, 863.
(3) Shaw, C. F. *Chem. Rev.* **1999**, *99*, 2589.
(4) Simon, T. M.; Kunishima, D. H.; Vibert, G. J.; Lorber, A. *Cancer* **1979**, *44*, 1965.
(5) Mirabelli, C. K.; Johnson, R. K.; Sung, C. M.; Faucette, L.; Muirhead, K.; Crooke, S. T. *Cancer Res.* **1985**, *45*, 32.
(6) Tiekink, E. R. T. *Inflammopharmacol.* **2008**, *16*, 138.
(7) Ott, I. *Coord. Chem. Rev.* **2009**, *253*, 1670.
(8) Che, C.-M.; Sun, R. W.-Y. *Chem. Commun.* **2011**, *47*, 9554.
(9) Bertrand, B.; Casini, A. *Dalton Trans.* **2014**, *43*, 4209.
(10) Bhabak, K. P.; Bhuyan, B. J.; Mugesh, G. *Dalton Trans.* **2011**, *40*, 2099.
(11) De Almeida, A.; Oliveira, B. L.; Correia, J. D. G.; Soveral, G.; Casini, A. *Coord. Chem. Rev.* **2013**, *257*, 2689.
(12) Dalla Via, L.; Nardon, C.; Fregona, D. *Future Med. Chem.* **2012**, *4*, 525.
(13) Bindoli, A.; Rigobello, M. P.; Scutari, G.; Gabbiani, C.; Casini, A.; Messori, L. *Coord. Chem. Rev.* **2009**, *253*, 1692.
(14) Gunatilleke, S. S.; Barrios, A. M. *J. Med. Chem.* **2006**, *49*, 3933.
(15) Weidauer, E.; Yasuda, Y.; Biswal, B. K.; Cherny, M.; James, M. N. G.; Bromme, D. *Biol. Chem.* **2007**, *388*, 331.
(16) Wang, Q. P.; Janzen, N.; Ramachandran, C.; Jirik, F. *Biochem. Pharmacol.* **1997**, *54*, 703.
(17) Krishnamurthy, D.; Karver, M. R.; Fiorillo, E.; Orru, V.; Stanford, S. M.; Bottini, N.; Barrios, A. M. *J. Med. Chem.* **2008**, *51*, 4790.
(18) Martins, A. P.; Marrone, A.; Ciancetta, A.; Galan Cobo, A.; Echevarria, M.; Moura, T. F.; Re, N.; Casini, A.; Soveral, G. *PLoS One* **2012**, *7*, e37435.
(19) Martins, A. P.; Ciancetta, A.; de Almeida, A.; Marrone, A.; Re, N.; Soveral, G.; Casini, A. *ChemMedChem* **2013**, *8*, 1086.
(20) Yang, J.; Merin, J.; Nakano, T.; Kato, T.; Kitade, Y.; Okamoto, T. *FEBS Lett.* **1995**, *361*, 89.
(21) Handel, M. L.; Watts, C. K.; deFazio, A.; Day, R. O.; Sutherland, R. L. *Proc. Natl. Acad. Sci. U. S. A.* **1995**, *92*, 4497.
(22) Stoyanov, J. V.; Brown, N. L. *J. Biol. Chem.* **2003**, *278*, 1407.
(23) Gabbiani, C.; Scaletti, F.; Massai, L.; Michelucci, E.; Cinellu, M. A.; Messori, L. *Chem. Commun.* **2012**, *48*, 11623.
(24) Kaps, L.; Biersack, B.; Mueller-Bunz, H.; Mahal, K.; Muenzner, J.; Tacke, M.; Mueller, T.; Schobert, R. *J. Inorg. Biochem.* **2012**, *106*, 52.
(25) Nose, Y.; Rees, E. M.; Thiele, D. J. *Trends Biochem. Sci.* **2006**, *31*, 604.
(26) Berg, J. M.; Shi, Y. G. *Science* **1996**, *271*, 1081.
(27) Laity, J. H.; Lee, B. M.; Wright, P. E. *Curr. Opin. Struct. Biol.* **2001**, *11*, 39.
(28) Matthews, J. M.; Sunde, M. *IUBMB Life* **2002**, *54*, 351.
(29) Krishna, S. S.; Majumdar, I.; Grishin, N. V. *Nucleic Acids Res.* **2003**, *31*, 532.
(30) Gamsjaeger, R.; Liew, C. K.; Loughlin, F. E.; Crossley, M.; Mackay, J. P. *Trends Biochem. Sci.* **2007**, *32*, 63.
(31) Andreini, C.; Bertini, I.; Cavallaro, G. *PLoS One* **2011**, *6*, e26325.
(32) Maret, W.; Li, Y. *Chem. Rev.* **2009**, *109*, 4682.
(33) Andreini, C.; Banci, L.; Bertini, I.; Rosato, A. *J. Proteome Res.* **2006**, *5*, 3173.
(34) Andreini, C.; Banci, L.; Bertini, I.; Rosato, A. *J. Proteome Res.* **2006**, *5*, 196.
(35) Maret, W. *Met. Ions Life Sci.* **2013**, *12*, 479.
(36) Pace, N. J.; Weerapana, E. *Biomolecules* **2014**, *4*, 419.
(37) Burdach, J.; O'Connell, M. R.; Mackay, J. P.; Crossley, M. *Trends Biochem. Sci.* **2012**, *37*, 199.
(38) Michalek, J. L.; Besold, A. N.; Michel, S. L. J. *Dalton Trans.* **2011**, *40*, 12619.
(39) Lee, S. J.; Michel, S. L. J. *Acc. Chem. Res.* **2014**, *47*, 2643.
(40) McMullen, M. R.; Pritchard, M. T.; Wang, Q. F.; Millward, C. A.; Croniger, C. M.; Nagy, L. E. *Gastroenterology* **2005**, *128*, 2066.
(41) Pavletich, N.; Pabo, C. *Science* **1991**, *252*, 809.
(42) Hudson, B. P.; Martinez-Yamout, M. A.; Dyson, H. J.; Wright, P. E. *Nat. Struct. Mol. Biol.* **2004**, *11*, 257.
(43) Handel, M. L.; Defazio, A.; Watts, C. K. W.; Day, R. O.; Sutherland, R. l. *Mol. Pharmacol.* **1991**, *40*, 613.
(44) Makino, Y.; Tanaka, H.; Dahlman Wright, K.; Makino, I. *Mol. Pharmacol.* **1996**, *49*, 612.
(45) Larabee, J. L.; Hocker, J. R.; Hanas, J. S. *Chem. Res. Toxicol.* **2005**, *18*, 1943.
(46) Franzman, M. A.; Barrios, A. M. *Inorg. Chem.* **2008**, *47*, 3928.
(47) De Paula, Q. A.; Mangrum, J. B.; Farrell, N. P. *J. Inorg. Biochem.* **2009**, *103*, 1347.
(48) Mendes, F.; Groessl, M.; Nazarov, A. A.; Tsybin, Y. O.; Sava, G.; Santos, I.; Dyson, P. J.; Casini, A. *J. Med. Chem.* **2011**, *54*, 2196.
(49) Laskay, Ü. A.; Garino, C.; Tsybin, Y. O.; Salassa, L.; Casini, A. *Chem. Commun.* **2015**, *51*, 1612.
(50) Jacques, A.; Mettra, B.; Lebrun, V.; Latour, J.-M.; Sénèque, O. *Chem.—Eur. J.* **2013**, *19*, 3921.
(51) Sénèque, O.; Bourlès, E.; Lebrun, V.; Bonnet, E.; Dumy, P.; Latour, J.-M. *Angew. Chem., Int. Ed.* **2008**, *47*, 6888.
(52) Jacques, A.; Latour, J.-M.; Sénèque, O. *Dalton Trans.* **2014**, *43*, 3922.
(53) Hollis, L. S.; Lippard, S. J. *J. Am. Chem. Soc.* **1983**, *105*, 4293.
(54) Nakamoto, K. *J. Phys. Chem.* **1960**, *64*, 1420.
(55) Messori, L.; Abbate, F.; Marcon, G.; Orioli, P.; Fontani, M.; Mini, E.; Mazzei, T.; Carotti, S.; O'Connell, T.; Zanello, P. *J. Med. Chem.* **2000**, *43*, 3541.
(56) Hogg, R.; Wilkins, R. *J. Chem. Soc.* **1962**, Jan, 341.
(57) Holyer, R.; Hubbard, C.; Kettle, S.; Wilkins, R. *Inorg. Chem.* **1966**, *5*, 622.
(58) Binstead, R.; Zuberbühler, A. *SPECFIT Global Analysis System*, version 3.0; Spectrum Software Associates: Marlborough, MA, 2000.
(59) Bau, R. *J. Am. Chem. Soc.* **1998**, *120*, 9380.
(60) Urig, S.; Fritz-Wolf, K.; Reau, R.; Herold-Mende, C.; Toth, K.; Davioud-Charvet, E.; Becker, K. *Angew. Chem., Int. Ed.* **2006**, *45*, 1881.
(61) Bachman, R. E.; Bodolosky-Bettis, S. A.; Pyle, C. J.; Gray, M. A. *J. Am. Chem. Soc.* **2008**, *130*, 14303.
(62) Abram, U.; Mack, J.; Ortner, K.; Muller, M. *J. Chem. Soc., Dalton Trans.* **1998**, No. No. 6, 1011.
(63) Millis, K.; Weaver, K.; Rabenstein, D. *J. Org. Chem.* **1993**, *58*, 4144.
(64) Mazid, M. A.; Razi, M. T.; Sadler, P. J.; Greaves, G. N.; Gurman, S. J.; Koch, M. H. J.; Phillips, J. C. *J. Chem. Soc., Chem. Commun.* **1980**, No. No. 24, 1261.
(65) Elder, R. C.; Ludwig, K.; Cooper, J. N.; Eidsness, M. K. *J. Am. Chem. Soc.* **1985**, *107*, 5024.

DOI: 10.1021/acs.inorgchem.5b00360
Inorg. Chem. 2015, 54, 4104−4113

(66) Xu, Y.; Wilcox, D. E. *J. Am. Chem. Soc.* **1998**, *120*, 7375.
(67) Shaw, C.; Cancro, M.; Witkiewicz, P.; Eldridge, J. *Inorg. Chem.* **1980**, *19*, 3198.
(68) Witkiewicz, P.; Shaw, C. *J. Chem. Soc., Chem. Commun.* **1981**, 1111.
(69) Sies, H. *Free Radical Biol. Med.* **1999**, *27*, 916.
(70) Goulet, P. J. G.; Lennox, R. B. *J. Am. Chem. Soc.* **2010**, *132*, 9582.
(71) Barngrover, B. M.; Aikens, C. M. *J. Am. Chem. Soc.* **2012**, *134*, 12590.
(72) Đurović, M. D.; Bugarčić, Ž. D.; Heinemann, F. W.; van Eldik, R. *Dalton Trans.* **2014**, *43*, 3911.
(73) Spell, S. R.; Farrell, N. P. *Inorg. Chem.* **2015**, *54*, 79.
(74) Serratrice, M.; Edafe, F.; Mendes, F.; Scopelliti, R.; Zakeeruddin, S. M.; Graetzel, M.; Santos, I.; Cinellu, M. A.; Casini, A. *Dalton Trans.* **2012**, *41*, 3287.
(75) Riddles, P. W.; Blakeley, R. L.; Zerner, B. *Methods Enzymol.* **1983**, *91*, 49.
(76) Proux, O.; Nassif, V.; Prat, A.; Ulrich, O.; Lahera, E.; Biquard, X.; Menthonnex, J. J.; Hazemann, J. L. *J. Synchrotron Radiat.* **2006**, *13*, 59.
(77) Ravel, B.; Newville, M. *J. Synchrotron Radiat.* **2005**, *12*, 537.

DOI: 10.1021/acs.inorgchem.5b00360
Inorg. Chem. 2015, 54, 4104−4113